



Disparate phenotypic effects from the knockdown of various *Trypanosoma brucei* cytochrome c oxidase subunits

Anna Gnipová^{a,b}, Brian Panicucci^a, Zdeněk Paris^{a,1}, Zdeněk Verner^{a,c}, Anton Horváth^b, Julius Lukeš^{a,c}, Alena Zíková^{a,c,*}

^a Institute of Parasitology, Biology Centre, České Budějovice, Czech Republic

^b Faculty of Science, Comenius University, Bratislava, Slovakia

^c Faculty of Science, University of South Bohemia, České Budějovice, Czech Republic

ARTICLE INFO

Article history:

Received 23 March 2012

Received in revised form 27 April 2012

Accepted 28 April 2012

Available online 5 May 2012

Keywords:

Trypanosoma

RNA interference

Mitochondrion

Respiratory complexes

Cytochrome c oxidase

ABSTRACT

The *Trypanosoma brucei* cytochrome c oxidase (respiratory complex IV) is a very divergent complex containing a surprisingly high number of trypanosomatid-specific subunits with unknown function. To gain insight into the functional organization of this large protein complex, the expression of three novel subunits (TbCOX VII, TbCOX X and TbCOX 6080) were down-regulated by RNA interference. We demonstrate that all three subunits are important for the proper function of complex IV and the growth of the procyclic stage of *T. brucei*. These phenotypes were manifested by the structural instability of the complex when these indispensable subunits were repressed. Furthermore, the impairment of cytochrome c oxidase resulted in other severe mitochondrial phenotypes, such as a decreased mitochondrial membrane potential, reduced ATP production via oxidative phosphorylation and redirection of oxygen consumption to the trypanosome-specific alternative oxidase, TAO. Interestingly, the inspected subunits revealed some disparate phenotypes, particularly regarding the activity of cytochrome c reductase (respiratory complex III). While the activity of complex III was down-regulated in RNAi induced cells for TbCOX X and TbCOX 6080, the TbCOX VII silenced cell line actually exhibited higher levels of complex III activity and elevated levels of ROS formation. This result suggests that the examined subunits may have different functional roles within complex IV of *T. brucei*, perhaps involving the ability to communicate between sequential enzymes in the respiratory chain. In summary, by characterizing the function of three hypothetical components of complex IV, we are able to assign these proteins as genuine and indispensable subunits of the procyclic *T. brucei* cytochrome c oxidase, an essential component of the respiratory chain in these evolutionary ancestral and medically important parasites.

© 2012 Elsevier B.V. All rights reserved.

1. Introduction

Trypanosoma brucei is a flagellated parasite of major medical and veterinary significance, causing Human African Trypanosomiasis and nagana in cattle [1]. It is a member of Excavata, a group comprised of important human parasites, such as *Giardia*, *Trichomonas*, *Naegleria*, *T. cruzi* and *Leishmania* ssp. [2]. *T. brucei* has become a model organism for these devastating protozoa because it is amenable to all reverse genetic approaches, which include gene knock-out by homologous recombination, inducible expression systems and RNA interference (RNAi) [3]. Furthermore, *T.*

brucei belongs to the class Kinetoplastida, which is named after the distinctive mitochondrial (mt) genomic structure located in its singular mitochondria. Kinetoplastida organisms are often regarded as primitive eukaryotes that have found fascinating ways to solve various problems presented to eukaryotes [4]. Thus, the pathogen *T. brucei* is now exploited for both the exploration of interesting biological processes of eukaryotic cells as well as deciphering its unique biology for future drug discovery.

The mitochondria of *T. brucei* houses several unique biological phenomena that have been extensively studied, including kinetoplast DNA structure and replication, RNA editing, and the respiratory pathway [5–8]. While all of these processes are essential, there is significant interest in the mechanism of respiration of the procyclic form (PF) of *T. brucei*, which resides in the digestive tract of its insect vector, the tse-tse fly [9]. During this life stage, the parasite can utilize its fully functional cytochrome-mediated respiratory pathway, which is comprised of a ubiquinone/ubiquinol pool, cytochrome c and four protein

* Corresponding author at: Biology Centre, Branišovská 31, 37005 České Budějovice, Czech Republic. Tel.: +420 387775482; fax: +420 385310388.

E-mail address: azikova@paru.cas.cz (A. Zíková).

¹ Present address: Department of Microbiology, The Ohio State University, Columbus, 43210 OH, USA.

complexes: complex I (NADH:ubiquinone reductase), II (SDH, succinate:ubiquinone reductase), III (*bc1*, ubiquinone:cytochrome *c* reductase), and IV (cytochrome *c* oxidase). This electron transport chain transfers electrons from the reduced NADH and FADH molecules to the final electron acceptor, an oxygen molecule. Concurrently, protons are pumped across the inner mt membrane by complexes III and IV to generate the essential mt membrane potential. This electrochemical gradient is then used by the F_0F_1 -ATP synthase to produce ATP by oxidative phosphorylation [10]. Interestingly, in addition to the conventional cytochrome-mediated respiratory pathway, the *T. brucei* mitochondrion utilizes a functionally distinct pathway to regenerate oxidized forms of NAD^+ molecules. This is achieved by the soluble alternative NADH dehydrogenase that passes electrons to ubiquinone [11]. These electrons can be further transferred to the plant-like alternative terminal oxidase (TAO) to reduce oxygen into water, though this process is not coupled with proton translocation [12,13]. Recently, comprehensive proteomic analyses have defined the composition of all the respiratory complexes [8], revealing the unique attributes of these macromolecular machines that consist of many protein subunits that have no homologs outside of Kinetoplastida. The most striking example of this divergence is respiratory complex IV, cytochrome *c* oxidase [14].

The cytochrome *c* oxidase complex was biochemically purified from three related trypanosomatid species *Crithidia fasciculata*, *Leishmania tarentolae* and *T. brucei*. To some extent, these purifications yielded overlapping sets of proteins, suggesting that in the trypanosomatid flagellates, the cytochrome *c* oxidase complex has at least 15 core nuclear-encoded subunits and three large mt-encoded subunits, a complexity similar to higher eukaryotic cytochrome *c* oxidases [14–16]. However, in contrast to these well conserved cytochrome *c* oxidase complexes, the *T. brucei* complex IV appears to be highly diverged, as only two of the nuclear-encoded subunits, COX VI and COX VIII, possess recognizable homology to the human subunits *coxVIb* and *coxIV*, respectively [14,17]. In addition to its core subunits, the *T. brucei* complex IV is transiently associated with an entourage of 18 proteins, most of them with unknown function [14]. While this divergence from the composition of oxidative phosphorylation complexes found in more publicized model species can be explained by the distant relationship of this ancient organism with higher eukaryotes, it is important to verify the true function of these hypothetical complex IV compatriots and begin to comprehend the alternative strategies employed by these medically important parasites.

Thus, in this study we characterized three proteins that have been shown to associate with trypanosomatid cytochrome *c* oxidase to various degrees: (i) Tb11.01.4702 (annotated as COX X in the geneDB database) was purified as a core subunit in each of the complexes isolated from *C. fasciculata*, *L. tarentolae* and *T. brucei*; (ii) Tb927.3.1410 (annotated as COX VII) is considered a core subunit in both the *C. fasciculata* and *L. tarentolae* complex, but is only transiently associated with the *T. brucei* complex; (iii) Tb927.8.6080–TbCOX 6080 (annotated as a hypothetical protein) was not detected in *C. fasciculata* or *L. tarentolae*; however, it was shown to transiently interact with the *T. brucei* complex [14,15,18]. The assignment of trypanosomatid cytochrome *c* oxidase subunits was based on the SDS-PAGE migration pattern observed for the purified subunits of the *C. fasciculata* cytochrome *c* oxidase complex. Since TbCOX VII and TbCOX X subunits show significant homology to *C. fasciculata* subunits VII and X, their nomenclature was made to acknowledge this attribute. However, the homologous *L. tarentolae* and *T. brucei* cytochrome *c* oxidase complexes do not display the same purification profiles as *C. fasciculata*. Since TbCOX 6080 subunit is not homologous to any known cytochrome *c* oxidase subunits, it was decided to use the geneDB identification number (e.g. Tb927.8.6080 = TbCOX 6080).

In order to explore the putative structural and functional associations of these subunits with the cytochrome *c* oxidase complex in *T. brucei*, we silenced all three genes by RNAi in the PF stage and examined the ensuing phenotypes. All three subunits are important for the structural integrity of the cytochrome *c* oxidase complex and their knockdowns caused severe phenotypes related to mt functions. Surprisingly, these subunits produced a disparate effect regarding the activity of the neighboring complex III and ROS production. These results suggest that all three subunits are genuine subunits of *T. brucei* complex IV, though they may have different functional roles, perhaps involving the ability to communicate between sequential enzymes in the respiratory chain.

2. Materials and methods

2.1. Construction of plasmids

To create the constructs for RNAi of TbCOX VII (Tb927.3.1410), TbCOX X (Tb11.01.4702) and TbCOX 6080 (Tb927.8.6080) transcripts, coding sequence (cds) fragments comprised of 486 base pairs (bp), 326 bp and 731 bp, respectively, were PCR amplified using the oligonucleotides listed below. The resulting PCR fragments were then cloned into the p2T7-177 plasmid [19] using XhoI and BamHI restriction sites (underlined).

TbCOX VII	Fw – 5' <u>CTCGAGCCCTTGGTGTGTTG</u>
	Rev – 5' <u>GGATCCGGCAGGAATATAGAA</u>
TbCOX X	Fw – 5' <u>CTCGAGGTTGCGTGTGCTTGC</u>
	Rev – 5' <u>GGATCCTACCAGCCGGATGG</u>
TbCOX 6080	Fw – 5' <u>CTCGAGCATCTAGTATGGCTG</u>
	Rev – 5' <u>GGATCCATATGGGCATACCAT</u>

2.2. Cell growth, transfection and RNAi induction

PF *T. brucei* strain 29.13 cells are transgenic for both the T7 RNA polymerase and the tetracycline (tet) repressor. Grown *in vitro* at 27°C in SDM-79 medium containing hemin (7.5 mg/ml) and 10% fetal bovine serum, these cells were used as the parental cell line for the RNAi transfections. The RNAi plasmids containing opposing T7 promoters regulated by tet were linearized with NotI and stably transfected into the minichromosome 177 bp repeat region. The synthesis of double-stranded (ds) RNA in clonal cell lines was induced by the addition of 1 µg/ml tet to the medium. Growth curves were generated over a period of 7 days by measuring the cell density of tet treated and untreated cell cultures using the Z2 cell counter (Beckman Coulter Inc.). Throughout the experiment, cells were split daily to ensure that they remained within their exponential growth phase of 10^6 – 10^7 cells/ml.

2.3. Northern blot analysis

A total of 10^8 uninduced and RNAi induced exponentially growing cells were harvested at appropriate time points and the total RNA was extracted with TriReagent (MRC), according to the instructions provided by the manufacturer. The RNA samples were resolved on a 1% agarose gel and transferred to a nitrocellulose membrane. Prior to blotting, the rRNAs for each sample were stained with ethidium bromide and visualized on the AlphaImager HP gel documentation system (Cell Biosciences) as a loading control. The same cds fragments used to generate each RNAi were labeled with [α - 32 P] dATP using the DecaLabel DNA labeling kit (Fermentas) and used as a probe. Hybridization of the probe to gene specific transcripts was performed using standard procedures, chiefly using a sodium phosphate buffer and hybridizing at 55°C. The radioactive signal from the blots was captured on GE Healthcare storage phosphor screens and the autoradiograms were analyzed

by densitometry using the Typhoon phosphorImager and ImageQuant software.

2.4. SDS-PAGE, 2D BN/Tricine SDS PAGE and Western blot analysis

Cleared whole cell or mt lysates fractionated on 12% SDS-PAGE gels were blotted onto a PVDF membrane and probed with polyclonal rabbit antibodies against *L. tarentolae* cytochrome *c* oxidase subunit IV (trCOIV) [20], *T. brucei* complex IV subunit VI (COVI) [21], or mt RNA binding protein 1 (MRP1) [22]. All of these polyclonal antibodies were used at a 1:500 dilution and the targeted proteins were visualized using the ECL system (Roche). The abundance of the immunodetected proteins was analyzed by densitometry (ImageQuant™ software, GE Healthcare) and normalized to the loading control. The intensity of each band is represented as a percentage of the uninduced sample, which was set as 100%.

Two dimensional (2D) PAGE analysis was performed by first fractionating 100 µg of mt lysate on a 6% BN PAGE gel, which was then further resolved on a 10% Tricine-SDS-PAGE gel. After electrophoresis, the gel was stained with Coomassie Brilliant Blue (G-250) to visualize mt respiratory complexes or transferred onto a nitrocellulose membrane and probed with an anti-trCOIV antibody.

2.5. In vitro and in gel activity measurements of respiratory complexes

Mt vesicles from 5×10^8 cells were isolated by hypotonic cell lysis, as described previously [21], and stored as pellets at -70°C . These mitochondria were then lysed with 2% dodecyl maltoside and the cytochrome *c* oxidase activity was determined *in vitro* by measuring the change in absorbance of cytochrome *c* as it becomes oxidized after passing its electrons to complex IV [21]. Cytochrome *c* reductase activity was determined in a similar way, this time the reduction of cytochrome *c* was measured when reduced decylubiquinone (Sigma) was added as an electron donor and complex III transferred these electrons to cytochrome *c*. In parallel, the same dodecyl maltoside lysed mitochondria samples were resolved (100 µg of protein per lane) on a 3–12% deep blue native (BN) PAGE gel and the cytochrome *c* oxidase activity was detected by an in-gel assay. The enzymatic activity of complex IV causes the native complex to be stained a dark blue as the electron acceptor 3,3'-diaminobenzidine is precipitated when it becomes reduced [23]. The enzymatic activities of complexes II and V were detected as described in [8,24].

2.6. FACS analysis of cells stained by TRME and DCFH-DA

To measure the changes in mt membrane potential, a 1 ml culture of mid-log phase cells was stained with 125 nM tetramethylrhodamine ethyl ester (TMRE, Molecular Probes) for 30 min at 27°C . These cells were then harvested, washed with an isotonic solution suitable for flow cytometry and then analyzed for red fluorescence by a flow cytometer (BD FACSCanto II). Twenty thousand events were measured for each experiment. The data was analyzed by FACSDiva Version 6.1.3 software and the values, representing the median of red fluorescence intensity, were expressed as a percentage of the uninduced cells, which were set as 100%.

Reacting oxygen species were measured using 2',7'-dichlorofluorescein diacetate (DCFH-DA, Sigma). DCFH-DA is a non-fluorescent dye that diffuses across the cell membrane and is retained as it becomes hydrolyzed intracellularly to form DCFH. In the presence of ROS, DCFH is rapidly oxidized to create the highly fluorescent compound, dichlorofluorescein. The uninduced and induced cells were incubated with 10 µM DCFH-DA for 30 min at 27°C as described in [25]. The cells were then washed once with

PBS-G and analyzed by FACS. Ten thousand events were measured in each experiment and the resulting data were analyzed using with Cyflogic™ software (CyFlo Ltd., Finland).

2.7. ATP production assay

ATP production was measured as described previously [26]. Briefly, a crude mt preparation from the untreated and tet treated RNAi cells was obtained by digitonin extraction. ATP production was then induced by the addition of 67 µM ADP and 5 mM of one of the substrates for the oxidative phosphorylation pathway (succinate) or for substrate phosphorylation (pyruvate and α -ketoglutarate). Specific inhibitors against succinate dehydrogenase (6.7 mM malonate) and the ADP/ATP carrier (33 µg/ml atractyloside) were preincubated with the enriched mitochondria samples for 10 min on ice to suppress oxidative phosphorylation. The resulting concentrations of ATP were determined by using the ATP Bioluminescence Assay Kit HS II (Roche) and a microplate luminometer (Orion II).

2.8. Measurement of oxygen consumption

Logarithmically growing cells were harvested, washed and resuspended in 1 ml of SDM-79 medium at a concentration of 2×10^7 cells ml $^{-1}$. Oxygen consumption at 27°C was determined with a Clark-type polarographic electrode (1302 Microcathode Oxygen Electrode, Strathkelvin Instruments). The specific inhibitors, potassium cyanide (KCN) for cytochrome *c* oxidase and salicylhydroxamic acid (SHAM) for trypanosomatid alternative oxidase, were added in 2 min intervals at final concentrations of 0.1 mM and 0.03 mM, respectively. Background respiration was determined after collectively adding KCN and SHAM. This value was then subtracted from the initial rate of respiration for both uninduced and RNAi induced cells respiring without either inhibitor, resulting in a value for total cellular oxygen consumption that was set to 100%. Each sample was then treated with 0.1 mM KCN to determine the percentage of oxygen consumed by TAO. The amount of respiration produced from respiratory complex IV was conversely calculated by subtracting the percentage of TAO oxygen consumption from the initial respiration rate that was normalized for background respiration.

3. Results

3.1. Inhibition of TbCOX VII, TbCOX X and TbCOX 6080 gene expression generates significant PF *T. brucei* growth defects

To evaluate the functional associations of all three of the selected putative subunits of cytochrome *c* oxidase, we constructed PF *T. brucei* cell lines in which the expression of Tb927.3.1410 (TbCOX VII), Tb11.01.4702 (TbCOX X) and Tb927.8.6080 (TbCOX 6080) can be inducibly silenced using RNAi. In all cases, RNAi was administered by the p2T7-177 construct [19], which regulates the expression of double stranded RNA in a tet-dependent manner, resulting in the RNAi mediated degradation of the target mRNA. After the addition of tet into the culture medium, the growth of the TbCOX VII cell line was strongly inhibited by day 3 (Fig. 1A). Meanwhile, the growth inhibition of the RNAi induced TbCOX X and TbCOX 6080 cells was less dramatic and slightly delayed as the growth phenotype did not become apparent until after the fourth day of tet induction (Fig. 1A). While the growth phenotype was delayed slightly longer for TbCOX 6080, the doubling time of these affected cells was significantly more inhibited than those of the RNAi induced TbCOX X cells from the same time period. The efficiency of the RNAi was confirmed by Northern blot analysis using transcript specific probes, demonstrating that the mRNA for TbCOX

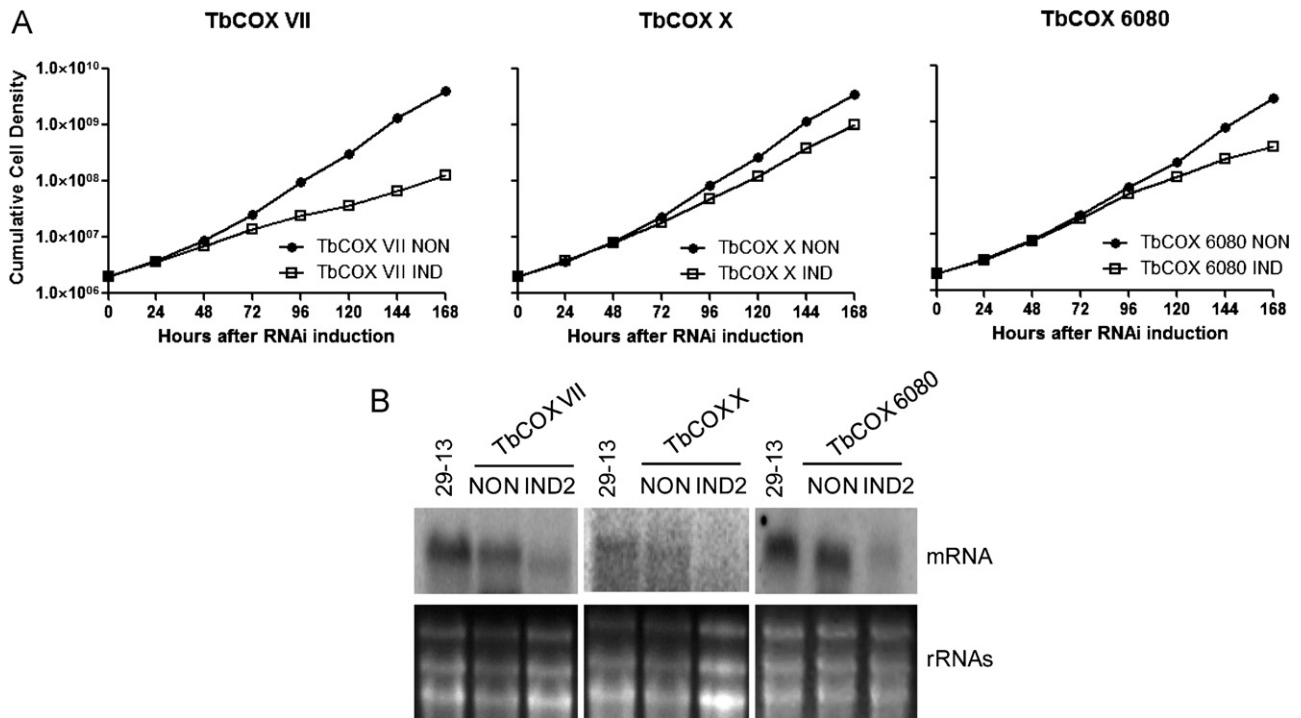


Fig. 1. Subunits TbCOX VII, TbCOX X and TbCOX 6080 are important for the *in vitro* growth of procyclic *T. brucei*. (A) Growth curves of the uninduced (NON) and tet induced (IND) TbCOX VII (left), TbCOX X (middle) and TbCOX 6080 (right) RNAi procyclic *T. brucei* cell lines. Cells were split everyday to maintain their exponential growth phase (between 10⁶ and 10⁷ cells/ml), thus the cumulative cell number represents the normalization of the daily cell density measurements by factoring in their dilution factor. Each graph is representative of the growth phenotype observed in three independent experiments. (B) Northern blot analysis of the corresponding mRNA (upper panel) for TbCOX VII, TbCOX X and TbCOX 6080 in the parental 29–13 cells, non-induced cells (NON) and cells 2 days upon induction of RNAi (IND2). As a loading control, the rRNAs (bottom panel) for each sample were stained with ethidium bromide and visualized with UV light.

VII, TbCOX X and TbCOX 6080 were all virtually eliminated after two days of RNAi induction (Fig. 1B). Based on the growth curve data, materials for all subsequent experiments involving TbCOX VII cells were collected on days 3 or 5 following RNAi induction, while the slightly delayed onset of the growth phenotype in the TbCOX X and TbCOX 6080 knockdown cells dictated that they be harvested at days 5 or 7 after the addition of tet.

3.2. Reduction of TbCOX VII, TbCOX X and TbCOX 6080 severely affects the function of cytochrome *c* oxidase

The biological function of complex IV is to transfer electrons from reduced cytochrome *c* to molecules of oxygen, while simultaneously contributing to the mt membrane potential by pumping H⁺ into the inner mt membrane space. To assess if the ability of complex IV to pump protons is compromised when these putative subunits are knocked-down, we measured the mt membrane potential of uninduced and RNAi induced cells using the fluorescent probe TMRE, which accumulates in the matrix of the mitochondria when there is an active membrane potential. The analysis of all three induced RNAi cell lines revealed a decrease in fluorescence intensity (Fig. 2), which is indicative of a reduced mt membrane potential. As expected, the strongest phenotype was observed in cells with downregulated TbCOX VII, where on day 3 after RNAi induction the mt membrane potential was decreased by ~60% relative to values obtained with the uninduced cells. The five day RNAi induced TbCOX X and TbCOX 6080 cells also demonstrated a decrease in their membrane potential. However, TbCOX X was only mildly affected (~25% inhibition), whereas TbCOX 6080 was inhibited almost as significantly as TbCOX VII (~50% inhibition) (Fig. 2).

Since the capacity of complex IV to pump protons is decreased in these knockdowns, we applied a BN gel-based assay to detect the

coordinated activity of the multi-subunit cytochrome *c* oxidase to transfer electrons to the artificial acceptor diaminobenzidine [21]. The mt lysates from uninduced and RNAi induced cells were fractionated on a BN gel and the cytochrome *c* oxidase activity was detected by histochemical staining (Fig. 3). The resulting dark blue activity band (~720 kDa) is in stark contrast to the faint staining of total protein seen in BN PAGE gels, as is evidenced by the intensity of the ~550 kDa band below it. In all RNAi induced cells, we observed a very strong decrease in the staining of this activity. To further corroborate this qualitative analysis, an *in vitro* assay was performed to

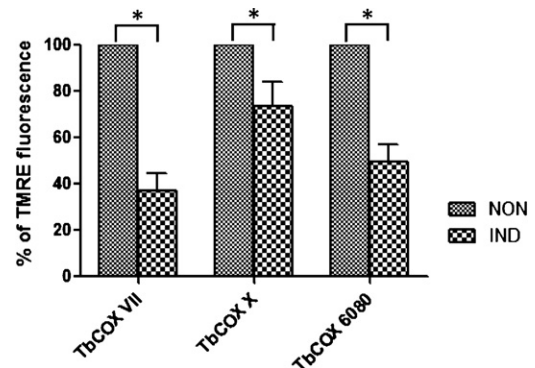


Fig. 2. Mitochondrial membrane potential is decreased following the reduction of TbCOX VII, TbCOX X and TbCOX 6080. Mt membrane potential was measured in both uninduced cells (NON, grey hatched bars) and tet induced RNAi cells (IND, black checkered bars) by flow cytometry after staining with TMRE. The fluorescence measurements for RNAi induced cells were obtained from day 3 for TbCOX VII and day 5 for TbCOX X and TbCOX 6080. The measured median values of red fluorescent intensity are represented as percentages of the uninduced sample, which was set to 100%. Data were obtained from at least three independent RNAi experiments and standard deviations are indicated. A Student's *t*-test analysis determined that the results are significant, with *P* values less than 0.05 (*).

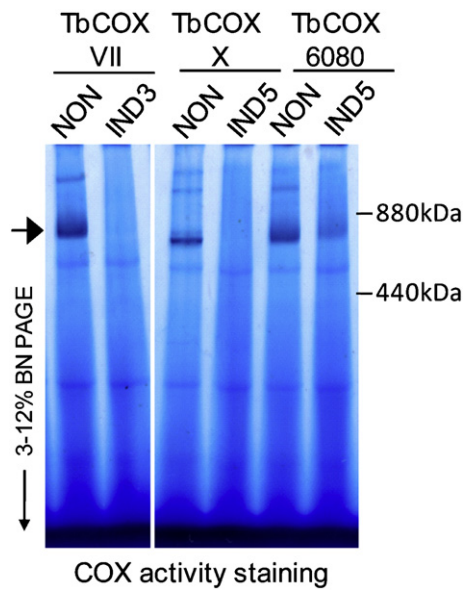


Fig. 3. Activity of the cyt *c* oxidase complex is affected upon depletion of TbCOX VII, TbCOX X and TbCOX 6080. In-gel *T. brucei* cyt *c* oxidase activity staining after the individual repression of subunits TbCOX VII (3 days after RNAi, IND3), TbCOX X and TbCOX 6080 (both 5 days after RNAi, IND5), compared to uninduced cells (NON). Mt preparations were solubilized using dodecyl maltoside and separated by 3–12% BN PAGE. The arrow points to bands visualized by the specific activity staining of cytochrome *c* oxidase, representing a complex of ~720 kDa. The sizes of high molecular weight markers (ferritin and its dimer, Sigma) are indicated on the right. This gel is representative of five independent experiments.

quantitatively measure the ability of complex IV to pass electrons to oxygen. As shown in Table 1, the specific cytochrome *c* oxidase activity was decreased by 67, 53 and 40% in TbCOX VII, TbCOX X and TbCOX 6080 RNAi induced cells, respectively, as compared to the uninduced cells. In summary, several independent assays demonstrate that both functions of cytochrome *c* oxidase, electron transfer and H⁺ transport, are significantly diminished after each of the three complex IV subunits are abated.

3.3. Cytochrome *c* oxidase loss of function is due to the impaired structural integrity of the complex

To ascertain if the loss of cytochrome *c* oxidase activity is due to the instability of the complex, we analyzed the composition of the complex when each of the putative subunits was knocked-down. This was achieved by separating dodecyl maltoside solubilized mt lysates by 2D BN/Tricine SDS PAGE and identifying cytochrome *c* oxidase subunits based on the migration patterns observed in previous work [20,21]. The position of the largest nuclear encoded subunit, trCOIV, in the 2D BN/Tricine–SDS PAGE gel was further verified by Western blot analysis using mt lysates of uninduced and induced TbCOX VII RNAi cells (Fig. 4A, right panel). While mitochondria from uninduced cells contain several of the observable

Table 1
Functional assay for cytochrome *c* reductase and cytochrome *c* oxidase activities.

Cell line	Cytochrome <i>c</i> reductase activities (%)	Cytochrome <i>c</i> oxidase activities (%)
TbCOX VII IND 5 days	123 ± 7	33 ± 5
TbCOX X IND 7 days	28 ± 3	47 ± 13
TbCOX 6080 IND 7 days	50 ± 4	60 ± 4

All activities were measured in mt lysates prepared from at least three independent experiments as described in the Experimental procedures. Activities in the RNAi induced cells are represented as a percentage of the uninduced cells, which are set to 100%. Mean values and standard deviations are indicated.

complex IV subunits, these proteins were significantly depleted or not detected at all in the same region of the gel containing the lysates of the RNAi induced cells (Fig. 4A and B, depicted area). These results suggest that the structural integrity of the cytochrome *c* oxidase complex is diminished after RNAi silencing of any of the examined subunits. Additional studies focusing on the individual components of the complex utilized specific antibodies already available against subunits trCOIV and COVI of the trypanosomatid respiratory complex IV. The steady-state abundance of these two core subunits in the total mt lysates of uninduced and RNAi induced cells was determined. As a consequence of the incomplete assembly of the cytochrome *c* oxidase complex, subunits trCOIV and COVI were drastically decreased (by 69% and 75%, respectively) in the induced TbCOX VII cells, significantly reduced (by 56% and 42%, respectively) in the cells depleted for TbCOX X and moderately depleted (by 36% and 29%, respectively) in the TbCOX 6080 induced cells (Fig. 4C). Thus, it appears that when any of these three investigated complex IV subunits are knocked-down, the stability of the complex is so severely affected that unincorporated trCOIV and COVI subunits become partially degraded.

3.4. Silencing of TbCOX VII, TbCOX X and TbCOX 6080 creates a disparate effect on the activity of cytochrome *c* reductase

Since the reduction of any of the three inspected complex IV subunits leads to a significantly decreased capacity of the complex to perform its normal functions, what are the implications for the rest of the respiratory chain complexes? To detect the ensuing effects of the loss of cytochrome *c* oxidase, the activities of other respiratory complexes were measured in each of the RNAi cell lines. The activities of respiratory complexes II and V were detected using BN and high resolution clear native gel electrophoresis, followed by in-gel specific activity staining. No significant differences in the activity and size of these complexes were observed (data not shown). Since no gel-based activity staining is available for the cytochrome *c* reductase complex, this activity was measured directly from mt lysates *in vitro*. Unexpectedly, the activity of this complex was slightly increased following the depletion of TbCOX VII, while it was considerably decreased in cells lacking the other two cytochrome *c* oxidase subunits, TbCOX X and TbCOX 6080 (Table 1). Since complex III is one of the major sites for reactive oxygen species (ROS) formation, its increased activity concurrent with the severe impairment of complex IV to transfer electrons, may result in higher intracellular ROS production. Therefore, it is plausible to hypothesize that a higher amount of ROS molecules will be formed in the induced TbCOX VII RNAi cell line. Indeed, on the third day of RNAi induction we detected a significant elevation of ROS molecules in this cell line (Fig. 5). However, it was not until day 5 post-tet induction that we finally observed a subtle increase in ROS production in the TbCOX 6080 cells, while no change was observed in the TbCOX X cells at this time. This result suggests that these subunits may have different complex IV functional roles in the mitochondrion of *T. brucei*, perhaps involving the cross-talk between sequential enzymes in the respiratory chain.

3.5. Diminished TbCOX VII, TbCOX X and TbCOX 6080 subunits effectively uncouples F₀F₁-ATP synthase

In PF *T. brucei*, respiratory complexes III and IV pump protons into the mt inner membrane space, resulting in a membrane potential that is then exploited by the coupled F₀F₁-ATP synthase to generate ATP by oxidative phosphorylation. Since this pathway depends on the proper function of all of the respiratory complexes, we investigated whether the generation of ATP *via* oxidative phosphorylation is affected in the complex IV RNAi induced cells. Indeed, we observed a significant decrease of ATP production by 85, 48

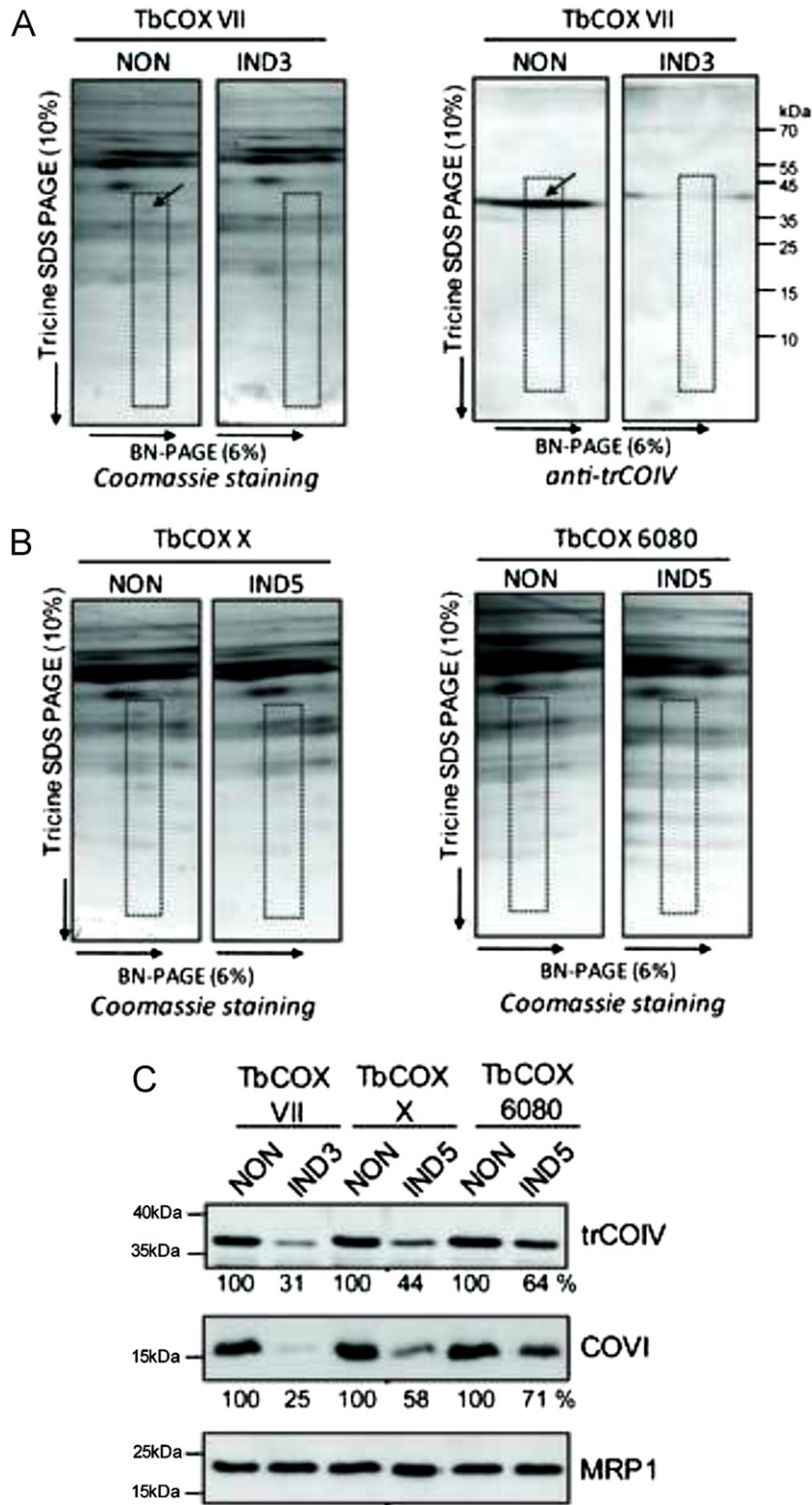


Fig. 4. Structural integrity of complex IV is affected by TbCOX VII, TbCOX X and TbCOX 6080 silencing. (A) 2D gel analysis of dodecyl maltoside-solubilized mitochondria of uninduced (NON) and day 3 induced (IND3) TbCOX VII RNAi cells. The 1st and 2nd dimensions were performed on a 6% BN gel and a 10% Tricine–SDS PAGE gel, respectively. The gel was stained with Coomassie Brilliant blue (left panel) or transferred onto a nitrocellulose membrane and probed with an anti-trCOIV antibody (right panel). The position of the largest nuclear encoded subunit, trCOIV, is indicated by an arrow. The area where the subunits of the cytochrome c oxidase complex migrate is indicated on the gel by a dashed box. The sizes of the molecular weight markers are indicated to the right of the Western blot. (B) 2D gel analysis of dodecyl maltoside-solubilized mitochondria of uninduced (NON) and day 5 induced (IND5) TbCOX X and TbCOX 6080 RNAi cells. The 2D BN/Tricine SDS PAGE gels were stained with Coomassie Brilliant blue. (C) Effects of TbCOX VII, TbCOX X and TbCOX 6080 RNAi on the steady-state abundance of the cytochrome c oxidase subunits trCOIV and COVI. Western blot analysis was performed on mt extracts obtained from uninduced RNAi cells (NON) and those induced with tet for 3 (IND3) or 5 (IND5) days. Each lane was loaded with 20 µg of total mt protein and the blots were immunodetected with a polyclonal antibody against trCOIV or COVI. Mt RNA binding protein (MRP1) served as a loading control. The numbers depicted underneath each panel represent the abundance of immunodetected protein expressed as a percentage of the uninduced samples after normalizing to the loading control. The sizes of the molecular weight markers are indicated on the left.

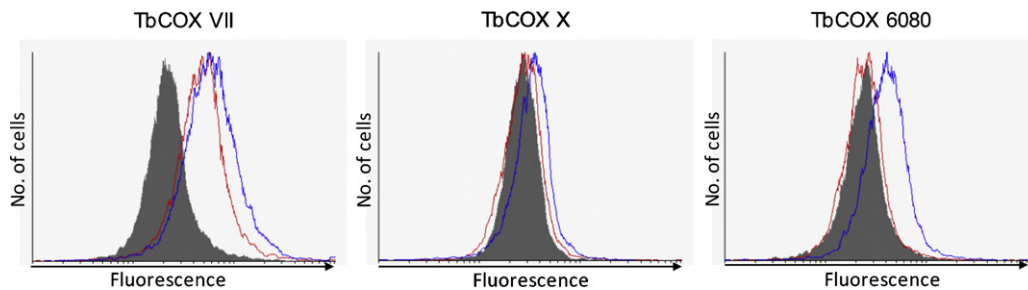


Fig. 5. ROS formation during TbCOX VII, TbCOX X and TbCOX 6080 RNAi. Measurement of intracellular reactive oxygen species in RNAi induced and uninduced cells using the ROS detection reagent DCFH-DA. Uninduced cells (shaded curve) and RNAi cells induced for 3 (red curve) or 5 (blue curve) days were analyzed by FACS analyses. The increase of the fluorescence intensity, most significantly witnessed in the TbCOX VII induced cells, corresponds to increased ROS formation that was observed in each of three independent assays. (For interpretation of the references to color in this figure caption, the reader is referred to the web version of the article.)

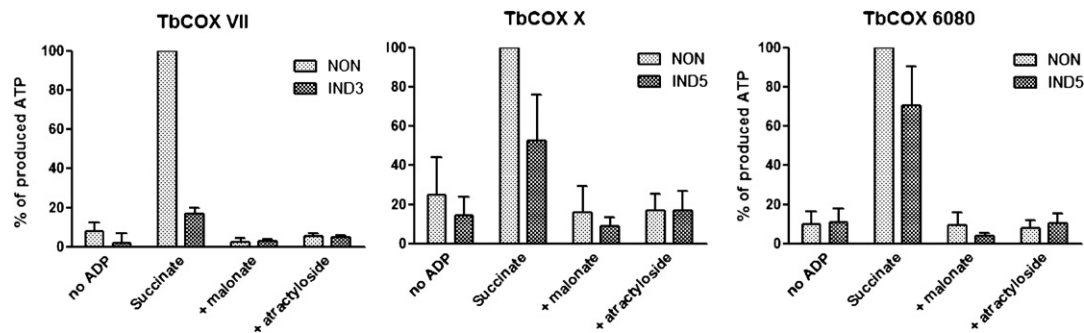


Fig. 6. ATP production by oxidative phosphorylation is severely reduced in mitochondria depleted for TbCOX VII, TbCOX X and TbCOX 6080. The *in vitro* generation of ATP was measured in digitonin-extracted mitochondria. The oxidative phosphorylation pathway was triggered by the addition of ADP and succinate. The level of ATP production in mitochondria isolated from uninduced RNAi cells stimulated with succinate without the presence of the specific inhibitors for succinate dehydrogenase (malonate) and the ADP/ATP carrier (atractyloside) was established as the reference and set to 100%. All other measurements in each panel are the mean values of each sample expressed as percentages of this reference sample, with the light grey bars representing the noninduced cells (NON) and the darker grey shaded bars representing RNAi samples induced for 3 (IND3) or 5 (IND5) days. “No ADP” serves as a control for the background production of ATP from the endogenous mt source of ADP. The data represent the average of three independent experiments and the standard deviations are indicated.

and 30% in RNAi induced TbCOX VII, TbCOX X and TbCOX 6080 cells, respectively (Fig. 6). Furthermore, this ATP synthesis was sensitive to malonate, an inhibitor of succinate dehydrogenase, and atractyloside, an inhibitor of the ATP/ADP translocator that provides the needed substrate for complex V. In addition to the oxidative phosphorylation pathway, which is triggered *in vitro* by succinate, there are two substrate phosphorylation pathways that are part of the incomplete citric acid cycle and the acetate-succinate CoA transferase/succinyl-CoA synthetase cycle [27]. While ATP generated specifically by oxidative phosphorylation was decreased in the inspected RNAi cells, neither of the substrate phosphorylation pathways were significantly affected in the RNAi interfered cells. Only a slight increase of ATP production by either substrate phosphorylation pathway was observed (data not shown). Taken together, these results show that TbCOX VII, TbCOX X and TbCOX 6080 directly affect ATP synthesis only *via* the oxidative phosphorylation pathway.

3.6. Depletion of TbCOX VII, TbCOX X and TbCOX 6080 causes a shift from cytochrome-mediated respiration to alternative oxidase

Interestingly, the mitochondrion of PF *T. brucei* cells is equipped with two oxygen-dependent terminal oxidases, namely the cytochrome *c* oxidase and TAO. Importantly, the electron flow from the cytochrome-mediated chain can be redirected to TAO when the former oxidase is disrupted. To verify this occurrence, the cells can be treated with drugs that selectively inhibit only one of these pathways, enabling one to distinguish between cytochrome *c* oxidase- and TAO-mediated oxygen consumption. After the addition of KCN, which selectively inhibits the activity of cytochrome *c*

oxidase, oxygen uptake decreased by about 70% in the uninduced cells, indicating that the majority of oxygen consumption occurs through the cytochrome mediated pathway in normal PF cells. This contrasts sharply with the RNAi induced cells, where there was a less dramatic decrease of KCN-sensitive oxygen consumption observed (Fig. 7). In particular, we measured only a 15% decrease in

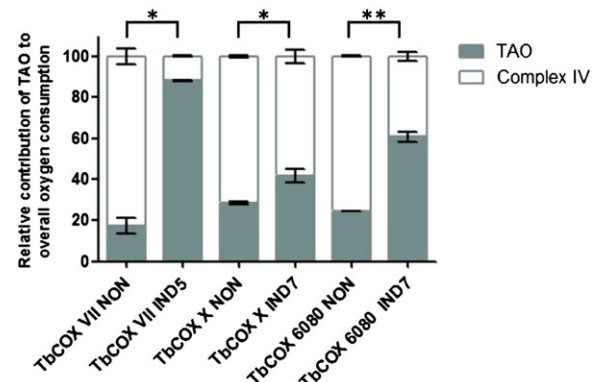


Fig. 7. Shift from cytochrome-mediated respiration to alternative oxidase respiration follows the repression of TbCOX VII, TbCOX X and TbCOX 6080. The oxygen consumption of uninduced and RNAi-induced cells incubated in SDM-79 medium at 27 °C was monitored with a Clark-type oxygen electrode. The graph depicts the percentage of total oxygen consumption by TAO. In this experiment, non-induced cells (NON) were compared with the TbCOX VII cell line induced with tet for 5 days (IND5) or the TbCOX X and TbCOX 6080 cell lines induced for 7 days (IND7). The mean and standard deviation values of three to four experiments are depicted. A Student's *t*-test analysis demonstrates that the results are significant with *P* values less than 0.05 (*) or less than 0.005 (**).

oxygen consumption when KCN was added to cells abated of TbCOX VII, which demonstrates that these cells have switched predominantly to TAO mediated respiration. A similar phenotype, although not as strong, was observed in cells with decreased TbCOX X and TbCOX 6080. These results are summarized in Fig. 7 by plotting the relative contribution to the overall cellular respiration by both the cytochrome *c* oxidase and TAO pathways. Importantly, the amount of respiration accounted for by TAO is proportional to the level of cytochrome *c* oxidase impairment produced by each of the RNAi cell lines.

4. Discussion

In this study, we presented evidence that TbCOX VII, TbCOX X and TbCOX 6080 are structurally and functionally important components of respiratory complex IV in *PF T. brucei*. This is a significant contribution to our understanding of the functional composition of a large protein complex, whose purification has revealed 15 core subunits and an additional 18 proteins not previously identified. This elaborate architecture implies that these additional proteins either directly complement the core subunits to comprise an unusual species-specific composition of cytochrome *c* oxidase or that they have transient interactions with the core complex and possess secondary functions. The increased complexity of cytochrome *c* oxidase in eukaryotes is often attributed to the increased need for regulation of this rate-limiting process in the cytochrome-mediated respiratory chain, which is even more important for this digenetic parasite whose complicated life cycle directly affects the regulation of its oxidative phosphorylation components [28,29]. However, an example of possible secondary functions is the association of cytochrome *c* oxidase with the MIX protein, which was shown to play a role in mt segregation and virulence in *L. major* [30]. This association adds further intricacy to the identification of the key functions of complex IV associated subunits and opens the possibility that cytochrome *c* oxidase is part of a larger membrane-bound multifunctional complex. Furthermore, recent studies of the individual complexes forming the electron transport chain in various protists revealed a surprisingly high number of lineage-specific subunits [24,31,32]. Therefore, the acquisition of unique components by these complexes can represent constructive neutral evolution, which might be responsible for the transformation of initially spurious associations into specialized essential functions of these subunits [33].

To gain insight into the function of the three novel complex IV candidate subunits, we prepared RNAi knockdowns for each of these subunits. While these knockdowns significantly decreased the level of the cognate RNA and the activity of cytochrome *c* oxidase, they generated phenotypes of various severity. This discrepancy could be explained by the possible difference in the turnover rate of subunits TbCOX VII, TbCOX X and TbCOX 6080; a claim currently difficult to verify in the absence of specific antibodies. Another alternative is that the built up complexity of the composition of complex IV in this protist allows for the function of TbCOX X and TbCOX 6080 to be complemented, to a limited extent, by other subunits.

Interestingly, it appears that the overall effect on the mt membrane potential most closely correlates with growth inhibition. For example, RNAi induced TbCOX X cells had significantly reduced cytochrome *c* oxidase activity *in vitro* (53%), but the mt membrane potential was only mildly affected and these cells displayed the weakest growth suppression. However, the TbCOX 6080 knockdown cells demonstrated less complex IV inactivation (40%), yet the mt membrane was more significantly decreased and the growth inhibition was more severe than the TbCOX X RNAi induced cells. This suggests that the overall viability of *PF T. brucei* grown *in vitro* is

more dependent on the mt membrane potential than on the ability of cytochrome *c* oxidase to transfer electrons in the oxidative phosphorylation pathway. This observation also complies with the fact that the infectious stage of this parasite sacrifices ATP produced from glycolysis to maintain the mt membrane potential by F₀F₁ ATPase [34].

One plausible explanation why RNAi of TbCOX VII produces the most debilitating growth phenotype incorporates the regulation of the oxidative phosphorylation pathway. We observe that the activity of cytochrome *c* oxidase is decreased when any of the studied subunits are repressed. Without complex IV, the electrons flowing through complex III are not capable of completely reducing the terminal acceptor molecule, oxygen, into water. Therefore, the flow of electrons from the conventional cytochrome-mediated pathway will be diverted to the alternative terminal oxidase, TAO, as we witnessed. The branching point between these two pathways is ubiquinone, so the diminished capability of complex IV in these circumstances must be communicated back to cytochrome *c* reductase in a manner that proportionately down-regulates its activity. Indeed, when TbCOX X or TbCOX 6080 are depleted, there is a significant decrease in the activity of both complex III and IV. However, with TbCOX VII ablation, complex IV activity is severely decreased while the activity of complex III is actually increased 20%. This suggests that TbCOX VII is responsible for the signaling mechanism that allows these two sequential respiratory complexes to communicate. Therefore, this loss of function results in the uncoordinated activity of complex III, resulting in an increased flow of electrons necessary to replenish the decreased mt membrane potential. However, this could decrease the overall fitness of the cell as complex III is also responsible for superoxide production [35]. This is validated by the significant increase in ROS production detected in the TbCOX VII RNAi cell line.

The mechanism of communication between complexes III and IV may depend on physical interactions, as yeast supercomplexes consisting of cytochrome *c* reductase and cytochrome *c* oxidase have been biochemically isolated [36]. This solid state model of the respiratory complexes would enhance substrate availability and allow electron flow to occur more efficiently [37]. The in-gel activity staining of *T. brucei* complexes III and IV on BN gels both correspond to a mobility of about 720 kDa, while their predicted sizes are only 237 kDa and 360 kDa, respectively [8]. While it is possible that these activity bands simply represent multimers of each individual complex, they could also represent an intact supercomplex of both complexes III and IV. This intriguing possibility needs to be further explored as previous results indirectly suggested that complexes III and IV do not assemble into supercomplexes [21].

While TbCOX 6080 is annotated as a hypothetical protein in the geneDB database, it has significant homology to the glycerophosphoryl diester phosphodiesterases (GDPD). In eukaryotes, membrane proteins that contain the GDPD motif and activity form a large family of proteins involved in phospholipid metabolism. The role of these enzymes is to hydrolyze deacylated phospholipids to generate glycerol-3-phosphate and the corresponding alcohol, thus participating in various biological functions involving pathogenesis and host immunity in bacteria, to scavenging phosphates in plants and yeast, as well as altering levels of oxygen consumption in mammalian cells [38]. While the available data cannot exclude or confirm the possibility that TbCOX 6080 plays a role in phospholipid catabolic processes, there is already a similar example of a respiratory complex anchoring a polypeptide of fatty acid metabolism. The acyl carrier protein is an essential component of complex I [39] and it affects the rate of cytochrome-mediated respiration in *T. brucei*, independently of the function of complex I [40]. Therefore, the future investigation of TbCOX 6080 could shed light on the increasing correlation between mt membrane composition and the regulation of oxidative phosphorylation.

The mt encoded subunits I, II and III form the functional core of all mt cytochrome *c* oxidases [41], but little is known about the function of the other associated proteins. It is predicted that these nuclear-encoded supplementary complex IV components are involved in the assembly of the complex, help maintain the structural integrity, or are involved in the regulation of the enzyme. While we have been able to further validate that TbCOX VII, TbCOX X and TbCOX 6080 are functional subunits of the PF *T. brucei* cytochrome *c* oxidase complex, additional studies need to be completed to tease apart the specific functions of these proteins. It is promising that this can be accomplished in the unique *T. brucei* model organism, which displays disparate phenotypes for each of the studied subunits.

Acknowledgements

We would like to thank the members of our laboratories for their meaningful discussions. Furthermore, the work contributed by A.Z. was supported by the Grant Agency of the Academy of Sciences (KJB500960901) and the EMBO Installation Grant No. 1965. J.L. is a Fellow of the Canadian Institute of Advanced Research and his research was supported by the Grant Agency of the Czech Republic 204/09/1667 and the Praemium Academiae. In addition, the Institute of Parasitology (project Z60220518) provided valuable resources to both A.Z. and J.L. Finally, results provided by A.H. were funded by the Scientific Grant Agency of the Slovak Ministry of Education and the Academy of Sciences 1/0393/09.

References

- [1] Simarro PP, Jannin J, Cattand P. Eliminating human African trypanosomiasis: where do we stand and what comes next? *PLoS Medicine* 2008;5:e55.
- [2] Hampl V, Hug L, Leigh JW, Dacks JB, Lang BF, Simpson AG, et al. Phylogenomic analyses support the monophyly of Excavata and resolve relationships among eukaryotic supergroups. *Proceedings of the National Academy of Sciences of the United States of America* 2009;106:3859–64.
- [3] Wirtz E, Leal S, Ochatt C, Cross GA. A tightly regulated inducible expression system for conditional gene knock-outs and dominant-negative genetics in *Trypanosoma brucei*. *Molecular and Biochemical Parasitology* 1999;99:89–101.
- [4] Simpson AG, Stevens JR, Lukes J. The evolution and diversity of kinetoplastid flagellates. *Trends in Parasitology* 2006;22:168–74.
- [5] Liu B, Liu Y, Motyka SA, Agbo EE, Englund PT. Fellowship of the rings: the replication of kinetoplast DNA. *Trends in Parasitology* 2005;21:363–9.
- [6] Stuart KD, Schnauffer A, Ernst NL, Panigrahi AK. Complex management: RNA editing in trypanosomes. *Trends in Biochemical Sciences* 2005;30:97–105.
- [7] Lukes J, Hashimi H, Zikova A. Unexplained complexity of the mitochondrial genome and transcriptome in kinetoplastid flagellates. *Current Genetics* 2005;48:277–99.
- [8] Acestor N, Zikova A, Dalley RA, Anupama A, Panigrahi AK, Stuart KD. *Trypanosoma brucei* mitochondrial respiratorome: composition and organization in procyclic form. *Molecular and Cell Proteomics* 2011;10:M110006908.
- [9] Vickerman K. Developmental cycles and biology of pathogenic trypanosomes. *British Medical Bulletin* 1985;41:105–14.
- [10] Besteiro S, Barrett MP, Riviere L, Bringaud F. Energy generation in insect stages of *Trypanosoma brucei*: metabolism in flux. *Trends in Parasitology* 2005;21:185–91.
- [11] Fang J, Beattie DS. Identification of a gene encoding a 54 kDa alternative NADH dehydrogenase in *Trypanosoma brucei*. *Molecular and Biochemical Parasitology* 2003;127:73–7.
- [12] Clarkson Jr AB, Bienen EJ, Pollakis G, Grady RW. Respiration of bloodstream forms of the parasite *Trypanosoma brucei brucei* is dependent on a plant-like alternative oxidase. *Journal of Biological Chemistry* 1989;264:17770–6.
- [13] Chaudhuri M, Ajayi W, Hill GC. Biochemical and molecular properties of the *Trypanosoma brucei* alternative oxidase. *Molecular and Biochemical Parasitology* 1998;95:53–68.
- [14] Zikova A, Panigrahi AK, Uboldi AD, Dalley RA, Handman E, F Stuart K. Structural and functional association of *Trypanosoma brucei* MIX protein with cytochrome *c* oxidase complex. *Eukaryotic Cell* 2008;7:1994–2003.
- [15] Speijer D, Muijsers AO, Dekker H, de Haan A, Breek CK, Albracht SP, et al. Purification and characterization of cytochrome *c* oxidase from the insect trypanosomatid *Crithidia fasciculata*. *Molecular and Biochemical Parasitology* 1996;79:47–59.
- [16] Horvath A, Berry EA, Huang LS, Maslov DA. *Leishmania tarentolae*: a parallel isolation of cytochrome bc(1) and cytochrome *c* oxidase. *Experimental Parasitology* 2000;96:160–7.
- [17] Speijer D, Breek CK, Muijsers AO, Groenevelt PX, Dekker H, de Haan A, et al. The sequence of a small subunit of cytochrome *c* oxidase from *Crithidia fasciculata* which is homologous to mammalian subunit IV. *FEBS Letters* 1996;381:123–6.
- [18] Horvath A, Kingan TG, Maslov DA. Detection of the mitochondrially encoded cytochrome *c* oxidase subunit I in the trypanosomatid protozoan *Leishmania tarentolae*. Evidence for translation of unedited mRNA in the kinetoplast. *Journal of Biological Chemistry* 2000;275:17160–5.
- [19] Wickstead B, Ersfeld K, Gull K. Targeting of a tetracycline-inducible expression system to the transcriptionally silent minichromosomes of *Trypanosoma brucei*. *Molecular and Biochemical Parasitology* 2002;125:211–6.
- [20] Maslov DA, Zikova A, Kyselova I, Lukes J. A putative novel nuclear-encoded subunit of the cytochrome *c* oxidase complex in trypanosomatids. *Molecular and Biochemical Parasitology* 2002;125:113–25.
- [21] Horvath A, Horakova E, Dunajcikova P, Verner Z, Pravdova E, Slapetova I, et al. Downregulation of the nuclear-encoded subunits of the complexes III and IV disrupts their respective complexes but not complex I in procyclic *Trypanosoma brucei*. *Molecular Microbiology* 2005;58:116–30.
- [22] Vondruskova E, van den Burg J, Zikova A, Ernst NL, Stuart K, Benne R, et al. RNA interference analyses suggest a transcript-specific regulatory role for mitochondrial RNA-binding proteins MRP1 and MRP2 in RNA editing and other RNA processing in *Trypanosoma brucei*. *Journal of Biological Chemistry* 2005;280:2429–38.
- [23] Jung C, Higgins CM, Xu Z. Measuring the quantity and activity of mitochondrial electron transport chain complexes in tissues of central nervous system using blue native polyacrylamide gel electrophoresis. *Analytical Biochemistry* 2000;286:214–23.
- [24] Zikova A, Schnauffer A, Dalley RA, Panigrahi AK, Stuart KD. The F(0)F(1)-ATP synthase complex contains novel subunits and is essential for procyclic *Trypanosoma brucei*. *PLoS Pathogen* 2009;5:e1000436.
- [25] Goldshmidt H, Matas D, Kabi A, Carmi S, Hope R, Michaeli S. Persistent ER stress induces the spliced leader RNA silencing pathway (SLS), leading to programmed cell death in *Trypanosoma brucei*. *PLoS Pathogen* 2010;6:e1000731.
- [26] Allemann N, Schneider A. ATP production in isolated mitochondria of procyclic *Trypanosoma brucei*. *Molecular and Biochemical Parasitology* 2000;111:87–94.
- [27] Schneider A, Bouzaidi-Tiali N, Chanez AL, Bulliard L. ATP production in isolated mitochondria of procyclic *Trypanosoma brucei*. *Methods of Molecular Biology* 2007;372:379–87.
- [28] Schnauffer A, Domingo GJ, Stuart K. Natural and induced dyskinetoplastic trypanosomatids: how to live without mitochondrial DNA. *International Journal for Parasitology* 2002;32:1071–84.
- [29] Matthews KR. The developmental cell biology of *Trypanosoma brucei*. *Journal of Cell Science* 2005;118:283–90.
- [30] Uboldi AD, Lueder FB, Walsh P, Spurck T, McFadden GI, Curtis J, et al. A mitochondrial protein affects cell morphology, mitochondrial segregation and virulence in *Leishmania*. *International Journal for Parasitology* 2006;36:1499–514.
- [31] Lapaille M, Escobar-Ramirez A, Degand H, Baurain D, Rodriguez-Salinas E, Coosemans N, et al. Atypical subunit composition of the chlorophycean mitochondrial F1FO-ATP synthase and role of Asa7 protein in stability and oligomycin resistance of the enzyme. *Molecular Biology and Evolution* 2010;27:1630–44.
- [32] Balabaskaran Nina P, Dudkina NV, Kane LA, van Eyk JE, Boekema EJ, Mather MW, et al. Highly divergent mitochondrial ATP synthase complexes in *Tetrahymena thermophila*. *PLoS Biology* 2010;8:e1000418.
- [33] Doolittle WF, Lukes J, Archibald JM, Keeling PJ, Gray MW. Comment on does constructive neutral evolution play an important role in the origin of cellular complexity? *Bioessays* 2011;33:427–9, doi:10.1002/bies.201100010.
- [34] Schnauffer A, Clark-Walker GD, Steinberg AG, Stuart K. The F1-ATP synthase complex in bloodstream stage trypanosomes has an unusual and essential function. *EMBO Journal* 2005;24:4029–40.
- [35] Muller FL, Liu Y, Van Remmen H. Complex III releases superoxide to both sides of the inner mitochondrial membrane. *Journal of Biological Chemistry* 2004;279:49064–73.
- [36] Schagger H, Pfeiffer K. Supercomplexes in the respiratory chains of yeast and mammalian mitochondria. *EMBO Journal* 2000;19:1777–83.
- [37] Vonck J, Schafer E. Supramolecular organization of protein complexes in the mitochondrial inner membrane. *Biochimica Et Biophysica Acta* 2009;1793:117–24.
- [38] Patton-Vogt J. Transport and metabolism of glycerophosphodiester produced through phospholipid decaylation. *Biochimica Et Biophysica Acta* 2007;1771:337–42.
- [39] Cronan JE, Fearnley IM, Walker JE. Mammalian mitochondria contain a soluble acyl carrier protein. *FEBS Letters* 2005;579:4892–6.
- [40] Guler JL, Kriegová E, Smith TK, Lukes J, Englund PT. Mitochondrial fatty acid synthesis is required for normal mitochondrial morphology and function in *Trypanosoma brucei*. *Molecular Microbiology* 2008;67:1125–42.
- [41] Cooper CE, Nicholls P, Freedman JA. Cytochrome *c* oxidase: structure, function, and membrane topology of the polypeptide subunits. *Biochemistry and Cell Biology* 1991;69:586–607.